Mineralogical Magazine, February 2012, Vol. 76(1), pp. 45–57

Davidlloydite, ideally $Zn_3(AsO_4)_2(H_2O)_4$, a new arsenate mineral from the Tsumeb mine, Otjikoto (Oshikoto) region, Namibia: description and crystal structure

F. C. Hawthorne[1,*], M. A. Cooper[1], Y. A. Abdu[1], N. A. Ball[1], M. E. Back[2] and K. T. Tait[2]

[1] Department of Geological Sciences, University of Manitoba, Winnipeg, Manitoba R3T 2N2, Canada
[2] Department of Natural History, Royal Ontario Museum, 100 Queen's Park, Toronto, Ontario M5S 2C6, Canada

[*Received 27 October 2011; Accepted 6 December 2011; Associate Editor: Allan Pring*]

ABSTRACT

Davidlloydite, ideally $Zn_3(AsO_4)_2(H_2O)_4$, is a new supergene mineral from the Tsumeb mine, Otjikoto (Oshikoto) region, Namibia. It occurs as elongated prisms (~10:1 length-to-width ratio) that are flattened on {010}, and up to $100 \times 20 \times 10$ μm in size. The crystals occur as aggregates (up to 500 μm across) of subparallel to slightly diverging prisms lying partly on and partly embedded in fine-grained calcioandyrobertsite. Crystals are prismatic along [001] and flattened on {010}, and show the forms {010} dominant and {100} subsidiary. Davidlloydite is colourless with a white streak and a vitreous lustre; it does not fluoresce under ultraviolet light. The cleavage is distinct on {010}, and no parting or twinning was observed. The Mohs hardness is 3–4. Davidlloydite is brittle with an irregular to hackly fracture. The calculated density is 3.661 g cm^{-3}. Optical properties were measured with a Bloss spindle stage for the wavelength 590 nm using a gel filter. The indices of refraction are $\alpha = 1.671$, $\beta = 1.687$, $\gamma = 1.695$, all ±0.002; the calculated birefringence is 0.024; $2V_{obs} = 65.4(6)^o$, $2V_{calc} = 70^o$; the dispersion is r < v, weak; pleochroism was not observed. Davidlloydite is triclinic, space group $P\bar{1}$, with $a = 5.9756(4)$, $b = 7.6002(5)$, $c = 5.4471(4)$ Å, $\alpha = 84.2892(9)$, $\beta = 90.4920(9)$, $\gamma = 87.9958(9)^o$, $V = 245.99(5)$ Å^3, $Z = 1$ and $a:b:c = 0.7861:1:0.7167$. The seven strongest lines in the X-ray powder diffraction pattern [listed as d (Å), I, (hkl)] are as follows: 4.620, 100, (011, $\bar{1}10$); 7.526, 71, (010); 2.974, 49, (200, $0\bar{2}1$); 3.253, 40, (021, 120); 2.701, 39, ($\bar{2}10$, 002, $\bar{1}\bar{2}1$); 5.409, 37, (001); 2.810, 37, (210). Chemical analysis by electron microprobe gave As_2O_5 43.03, ZnO 37.95, CuO 5.65, H_2O(calc) 13.27, sum 99.90 wt.%. The H_2O content and the valence state of As were determined by crystal structure analysis. On the basis of 12 anions with $H_2O = 4$ a.p.f.u., the empirical formula is $(Zn_{2.53}Cu_{0.39})_{\Sigma 2.92}As_{2.03}O_8(H_2O)_4$.

The crystal structure of davidlloydite was solved by direct methods and refined to an R_1 index of 1.51% based on 1422 unique observed reflections collected on a three-circle rotating-anode (Mo$K\alpha$ radiation) diffractometer equipped with multilayer optics and an APEX-II detector. In the structure of davidlloydite, sheets of corner-sharing ($As^{5+}O_4$) and (ZnO_4) tetrahedra are linked by $ZnO_2(H_2O)_4$ octahedra. The structure is related to that of parahopeite.

Keywords: Davidlloydite, new mineral species, arsenate, Tsumeb mine, Otjikoto (Oshikoto) region, Namibia, crystal structure, electron microprobe analysis, optical properties.

Introduction

The Tsumeb mine in the Otjikoto (Oshikoto) region of Namibia was a major source of Cu-Pb-Zn ores for much of the twentieth century (Weber and Wilson, 1977) and is well known for the large number of mineral species it has produced (Pinch and Wilson, 1977). Examination of a sample from the Charles Key Collection, purchased by the Royal Ontario Museum in 2003, resulted in the identification

* E-mail: frank_hawthorne@umanitoba.ca
DOI: 10.1180/minmag.2012.076.1.45

of a new hydrated zinc arsenate mineral. This mineral is named davidlloydite after David Lloyd (born 24 March 1943 in Bristol, England), a prominent mineral collector who was a prime mover in the re-opening of the Tsumeb mine for mineral collecting, and who has made significant contributions to mineralogy through extensive field collecting at many localities in the British Isles.

The new mineral and mineral name have been approved by the Commission on New Minerals, Nomenclature and Classification of the International Mineralogical Association (IMA 2011-053). The holotype specimen of davidlloydite has been deposited in the mineral collection of the Department of Natural History, Royal Ontario Museum, catalogue number M56120.

Occurrence

Davidlloydite was discovered on a sample from the Tsumeb mine, Otjikoto (Oshikoto) region, Namibia. It is associated with stranskiite, geminite, adamite–olivenite and calcioandyrobertsite, and is thought to have originated on the 4400-foot level of the mine in an area known as the third oxidation zone.

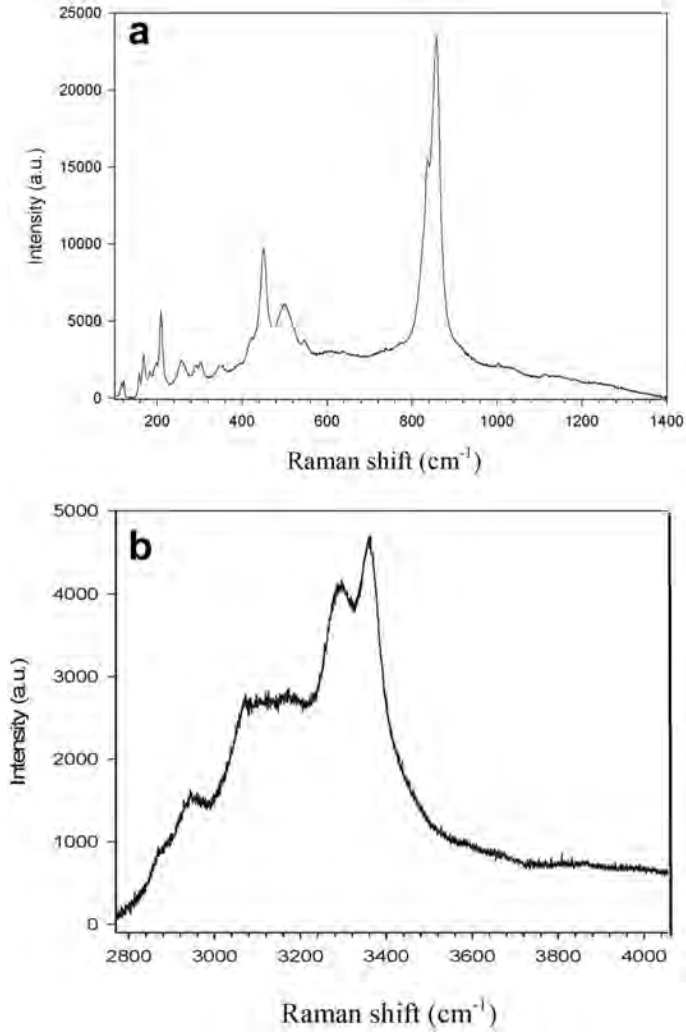

FIG. 1. The Raman spectrum of davidlloydite.

TABLE 1. Optical orientation (º) of davidlloydite.

	a	*b*	*c*
X	118.3	117.4	142.8
Y	142.7	56.1	77.3
Z	67.8	46.3	124.2

Physical properties

Davidlloydite crystals are elongated prisms (~10:1 length-to-width ratio) that are flattened on {010} and up to 100 × 20 × 10 μm in size. The crystals occur as aggregates (up to 500 μm across) of subparallel to slightly diverging prisms lying partly on and partly embedded in fine-grained calcioandyrobertsite. Crystals are prismatic along [001] and flattened on {010}, and show the forms {010} dominant, {100} subsidiary. Davidlloydite is colourless with a white streak and a vitreous to opalescent lustre; it does not fluoresce under ultraviolet light. The cleavage is distinct on {010}, and no parting or twinning was observed. The Mohs hardness is 3–4, and davidlloydite is brittle with an irregular to hackly fracture. The density was not measured due to the paucity of material. The calculated density is 3.661 g cm^{-3}. Optical properties were measured with a Bloss spindle stage for the wavelength 590 nm. The indices of refraction are $\alpha = 1.671$, $\beta = 1.687$, $\gamma = 1.695$, all ±0.002; $2V_{obs} = 65.4(6)^o$ (measured with a spindle stage, data processed using *Excalibr II*, Bartelmehs *et al.*, 1992), $2V_{calc} = 70^o$; the dispersion is r < v, weak. No pleochroism was observed; the optic orientation is given in Table 1.

TABLE 2. Chemical composition of davidlloydite.

Constituent	Mean (wt.%)	Range
As_2O_5	43.03(1.08)	41.18–43.95
ZnO	37.95(1.62)	35.86–40.23
CuO	5.65(0.68)	4.70–6.55
H_2O(calc.)	13.27	–
Total	99.90	–

Not detected: P, Mg, Mn, Fe, Al, Si, Na, Ca, V, Cr.

TABLE 3. X-ray powder diffraction data for davidlloydite.

I_{obs}	d_{obs}	d_{calc}	*h k l*
71	**7.526**	7.547	0 1 0
16	5.960	5.964	1 0 0
37	**5.409**	5.420	0 0 1
100	**4.620**	4.627	0 1 1
		4.600	$\bar{1}$ 1 0
25	4.200	4.208	0 $\bar{1}$ 1
10	3.999	4.031	$\bar{1}$ 0 1
		3.991	1 0 1
9	3.768	3.773	0 2 0
30	**3.635**	3.633	$\bar{1}$ 1 1
24	3.393	3.394	1 $\bar{1}$ 1
40	**3.253**	3.253	0 2 1
		3.241	1 2 0
49	**2.974**	2.982	2 0 0
		2.961	0 $\bar{2}$ 1
11	2.885	2.886	1 2 1
37	**2.810**	2.808	2 1 0
39b*	**2.701**	2.740	$\bar{2}$ 1 0
		2.710	0 0 2
		2.688	$\bar{1}$ $\bar{2}$ 1
20	2.626	2.636	0 1 2
		2.618	1 $\bar{2}$ 1
13	2.514	2.516	0 3 0
23	2.459	2.458	1 0 2
17	2.404	2.409	$\bar{1}$ 1 2
		2.402	2 $\bar{1}$ 1
2	2.299	2.302	$\bar{1}$ $\bar{1}$ 2
22	2.225	2.226	2 2 1
19	2.175	2.184	$\bar{1}$ 3 1
		2.172	$\bar{2}$ 2 1
6	2.138	2.137	$\bar{2}$ $\bar{2}$ 1
2	2.066	2.067	2 $\bar{2}$ 1
4b*	2.035	2.041	1 $\bar{3}$ 1
10	2.014	2.016	$\bar{2}$ 0 2
9	1.996	1.996	2 0 2
8	1.887	1.890	$\bar{2}$ 3 0
		1.887	0 4 0
		1.884	2 3 1
6	1.839	1.840	2 2 2
6	1.819	1.816	$\bar{2}$ 2 2
3	1.781	1.781	$\bar{1}$ 4 0
3	1.740	1.742	$\bar{2}$ $\bar{2}$ 2
		1.741	2 $\bar{3}$ 1
3	1.721	1.721	1 1 3
2	1.698	1.697	0 2 3
5	1.672	1.672	$\bar{1}$ $\bar{4}$ 1
		1.677	1 $\bar{3}$ 2

* The abbreviation b signifies a broad line.

TABLE 4. Summary of crystallographic, data collection and structure refinement information for davidlloydite.

a (Å)	5.9756(4)	Crystal size (μm)	20 × 20 × 80
b (Å)	7.6002(5)	Radiation/monochromater	Mo$K\alpha$/Graphite
c (Å)	5.4471(4)	No. of reflections	8846
α (º)	84.2892(9)	No. in Ewald sphere	2946
β (º)	90.4920(9)	No. unique reflections	1477
γ (º)	87.9958(9)	No. with ($F_o > 4\sigma F$)	1422
V (Å^3)	245.99(5)	R_{merge}%	0.91
Space group	$P\bar{1}$	R_1%	1.51
Z	1	wR_2%	4.13
d_{calc} (g cm^{-3})	3.661		
Cell content	$Zn_3(AsO_4)_2(H_2O)_4$		

$R_1 = \Sigma(|F_o| - |F_c|)/\Sigma|F_o|$.
$wR_2 = [\Sigma w(F_o^2 - F_c^2)^2/\Sigma w(F_o^2)^2]^{½}$, $w = 1/[\sigma^2(F_o^2) + (0.0139P)^2 + 0.34P]$ where $P = (\mathrm{Max}(F_o^2,0) + 2F_c^2)/3$.

Raman spectroscopy

The Raman spectrum of davidlloydite is shown in Fig. 1. In the 100−1200 cm^{-1} region, there is a prominent peak at 865 cm^{-1} and a strong but subsidiary band at 841 cm^{-1}, both of which may be assigned to As^{5+}−O stretching modes. Lower-energy peaks at 550 (w), 504 (m), 454 (s) and 420 (vw) cm^{-1} may be assigned to Zn−O stretching modes, and the numerous lower-energy bands may be assigned to collective lattice modes: 394 (vw), 353 (w), 305 (w), 294 (w), 258 (w), 211 (w), 200 (w), 182 (w), 170 (w), 163 (w) and 121 (doublet, vw). In the 2500−4000 cm^{-1} region, there is a broad envelope with significant structure, centred on ~3200 cm^{-1} that may be assigned to various stretching modes of the H_2O group.

Chemical composition

Davidlloydite was analysed using a Cameca SX-100 electron microprobe operating in wavelength-dispersive mode with an accelerating voltage of 15 kV, a specimen current of 10 nA and a beam diameter of 10 μm. Different crystals were used for the single-crystal structure refinement and chemical analysis. The standards used were adamite (As, Zn) and olivenite (Cu). The data were reduced and corrected by the *PAP* method of Pouchou and Pichoir (1985) and are given in Table 2 (mean of five determinations). The presence and quantity of H_2O groups were established by crystal-structure solution and refinement. In addition, Raman spectroscopy (Fig. 1) indicates a broad intense band in the region ~3200 cm^{-1}, which is indicative of H_2O. The empirical formula was calculated on the basis of 12 anions with H_2O = 4 a.p.f.u. (atoms per formula unit) as indicated by crystal-structure solution and refinement, giving $(Zn_{2.53}Cu_{0.39})_{\Sigma 2.92}As_{2.03}O_8(H_2O)_4$, and an ideal formula $Zn_3(AsO_4)_2(H_2O)_4$.

X-ray powder diffraction

X-ray powder-diffraction data were obtained using a Gandolfi attachment mounted on a Bruker D8 rotating-anode Discover SuperSpeed micro-powder diffractometer with a multi-wire 2D detector. Data (in Å for Cu$K\alpha$) are listed in Table 3. Unit-cell parameters refined from the powder data are as follows: a = 5.968(4), b = 7.589(4), c = 5.448(3) Å, α = 84.29(5)º, β = 90.38(4), γ = 88.01(5), V = 245.3(2) Å^3.

Crystal-structure solution and refinement

A crystal was attached to a tapered glass fibre and mounted on a Bruker D8 three-circle diffractometer equipped with a rotating-anode generator (Mo$K\alpha$), multilayer optics and an APEX-II detector. A total of 2946 intensities (those within the Ewald sphere) was collected to 60º2θ using 10 s per 0.2º frame, with a crystal-to-detector distance of 5 cm. Empirical absorption corrections (*SADABS*; Sheldrick, 2008) were applied and equivalent reflections were corrected for Lorentz, polarization and background effects, averaged and reduced to structure factors. The unit-cell dimensions were obtained by least-squares refinement of the positions of 6593 reflections with $I > 10\sigma I$ and are given in

TABLE 5. Atom coordinates and displacement parameters (Å^2) for davidlloydite.

Atom	*x/a*	*y/b*	*z/c*	U_{11}	U_{22}	U_{33}	U_{23}	U_{13}	U_{12}	U_{eq}
Zn(1)	0	½	½	0.01425(19)	0.01053(18)	0.01178(19)	−0.00034(12)	0.00126(12)	0.00005(13)	0.01224(12)
Zn(2)	0.23922(4)	0.10407(3)	0.81081(4)	0.01204(12)	0.01445(12)	0.01032(11)	−0.00186(8)	−0.00006(8)	0.00121(9)	0.01226(7)
As(1)	0.25896(3)	0.87032(3)	0.33696(4)	0.00945(10)	0.00940(10)	0.00869(10)	−0.00125(7)	0.00025(7)	0.00002(7)	0.00916(6)
O(1)	0.4813(3)	0.7644(2)	0.2259(3)	0.0119(7)	0.0140(7)	0.0204(8)	−0.0045(6)	0.0037(6)	0.0007(5)	0.0153(3)
O(2)	0.2996(3)	0.8972(2)	0.6354(3)	0.0200(8)	0.0144(7)	0.0096(7)	−0.0027(5)	−0.0011(5)	0.0007(6)	0.0146(3)
O(3)	0.0271(3)	0.7464(2)	0.3144(3)	0.0103(6)	0.0120(7)	0.0157(7)	0.0002(5)	−0.0012(5)	−0.0014(5)	0.0128(3)
O(4)	0.1952(3)	0.0630(2)	0.1674(3)	0.0209(8)	0.0116(7)	0.0105(7)	0.0010(5)	−0.0006(6)	0.0015(6)	0.0145(3)
O(5)	0.2229(3)	0.4010(2)	0.2726(3)	0.0253(9)	0.0134(7)	0.0155(8)	−0.0007(6)	0.0037(6)	0.0009(6)	0.0181(3)
O(6)	0.2711(3)	0.5420(2)	0.7834(4)	0.0190(8)	0.0162(8)	0.0270(9)	−0.0008(6)	0.0031(7)	−0.0009(6)	0.0208(3)
H(1)	0.211(6)	0.2762(14)	0.245(7)							0.039(10)
H(2)	0.232(7)	0.453(5)	0.101(3)							0.056(13)
H(3)	0.413(4)	0.481(5)	0.748(8)							0.058(13)
H(4)	0.325(7)	0.662(2)	0.791(8)							0.059(13)

Table 4, together with other information pertaining to data collection and structure refinement.

All calculations were done with the *SHELXTL PC (Plus)* system of programs; *R* indices are of the form given in Table 4 and are expressed as percentages. The structure was solved in the space group $P\bar{1}$ by direct methods and refined to convergence by full-matrix least-squares methods with anisotropic-displacement parameters for all atoms. At the later stages of refinement, difference-Fourier maps showed weak density maxima approximately 1 Å from the O(5) and O(6) anions that incident bond-valence sums indicate are H_2O groups. These maxima were entered into the structure model as H atoms and their parameters were refined with the soft constraint that the O−H distance be approximately 0.98 Å. The structure converged to a final R_1 index of 1.51%. Refined atom coordinates and anisotropic-displacement parameters are listed in Table 5, selected interatomic distances are given in Table 6, and bond valences, calculated with the parameters of Brown and Altermatt (1985), are given in Table 7. A table of structure factors and a crystallographic information file are available at www.minersoc.org/pages/e_journals/dep_mat.html.

Crystal structure

Coordination of cations

In the structure of davidlloydite, the *As* site is tetrahedrally coordinated by four O anions at a mean distance of 1.687 Å, which is characteristic of As^{5+} [e.g. adamite: 1.681 Å (Hawthorne, 1976*a*); scorodite: 1.680 Å (Hawthorne, 1976*b*)], and the site-scattering is in accord with full occupancy of the site by As. There are two *Zn* sites with different coordination numbers, which are occupied primarily by Zn with minor Cu^{2+} (Table 2). The *Zn*(1) site is octahedrally coordinated by two O^{2-} anions and four (H_2O) groups with a <*Zn*−O> distance of 2.112 Å. The *Zn*(2) site is tetrahedrally coordinated by O^{2-} anions with a <*Zn*−O> distance of 1.970 Å. The [4+2] distortion observed for the *Zn*(1) octahedron suggests that the Cu measured by electron-microprobe analysis (Table 2) is ordered at the octahedrally coordinated *Zn*(1) site. The crystal analysed by electron-microprobe analysis can be described by the site-specific formula $^{[6]}(Zn_{0.6}Cu_{0.4})^{[4]}Zn_2(AsO_4)_2(H_2O)_4$.

TABLE 6. Selected interatomic distances (Å) and angles (°) in davidlloydite.

Zn(1)–O(3) ×2	2.050(2)	*Zn*(2)–O(1)	1.978(2)
Zn(1)–O(5) ×2	2.005(2)	*Zn*(2)–O(2)	1.944(2)
Zn(1)–O(6) ×2	2.281(2)	*Zn*(2)–O(3)	1.998(2)
<*Zn*(1)–O>	2.112	*Zn*(2)–O(4)	1.958(2)
		<*Zn*(2)–O>	1.970
As–O(1)	1.678(2)		
As–O(2)	1.675(2)		
As–O(3)	1.713(2)		
As–O(4)	1.682(2)		
<*As*–O>	1.687		
O(5)–H(1)	0.980(1)	H(1)···O(4)	1.720(4)
O(5)–H(2)	0.980(1)	H(2)···O(6)	1.814(4)
O(5)–H(1)···O(4)	175(3)		
O(5)–H(2)···O(6)	176(4)		
O(6)–H(3)	0.980(1)	H(3)···O(1)	1.94(3)
O(6)–H(4)	0.980(1)	H(4)···O(2)	1.90(3)
O(6)–H(3)···O(1)	135(3)		
O(6)–H(4)···O(2)	143(4)		

Anion identities and hydrogen bonding

There are six crystallographically distinct anions, O(1)–O(6) (Table 5). Inspection of the bond-valence table (Table 7) shows that the bond valence incident at O(1) to O(4), omitting any contribution from H, is $\geqslant$1.75 vu, indicating that these anions are O^{2-}. The corresponding bond-valence incident at O(5) and O(6) is 0.44 and 0.21 vu, indicating that both O(5) and O(6) are H_2O groups. In accord with this conclusion, four H sites were identified in difference-Fourier maps close to the O(5) and O(6) sites and refined in the final stages of structure refinement. The resulting hydrogen-bond arrangements are given in Table 6. The O(4) and O(6) anions are acceptor anions for hydrogen bonds from the donor O(5) anion, and the O(1) and O(2) anions are acceptor anions for hydrogen bonds from the donor O(6) anion. The resulting incident bond-valence sums at all of the anions in the structure accord with the valence-sum rule to within ±0.05 vu or less (Table 7) and the anion part of the formula is $O_8(H_2O)_4$ for $Z = 1$.

Bond topology

A very unusual aspect of the structure of davidlloydite is its relation to the structure of

TABLE 7. Bond-valence* table for davidlloydite.

	Zn(1)	*Zn*(2)	*As*	Σ	H(1)	H(2)	H(3)	H(4)	Σ
O(1)		0.48	1.27	1.75			0.2		1.95
O(2)		0.52	1.28	1.80				0.2	2.00
O(3)	$0.39^{\times 2}\downarrow$	0.45	1.16	2.00					2.00
O(4)		0.50	1.26	1.76	0.2				1.96
O(5)	$0.44^{\times 2}\downarrow$			0.44	0.8	0.8			2.04
O(6)	$0.21^{\times 2}\downarrow$			0.21		0.2	0.8	0.8	2.01
Σ	2.08	1.95	4.97		1.00	1.00	1.00	1.00	

* See Brown and Altermatt (1985).

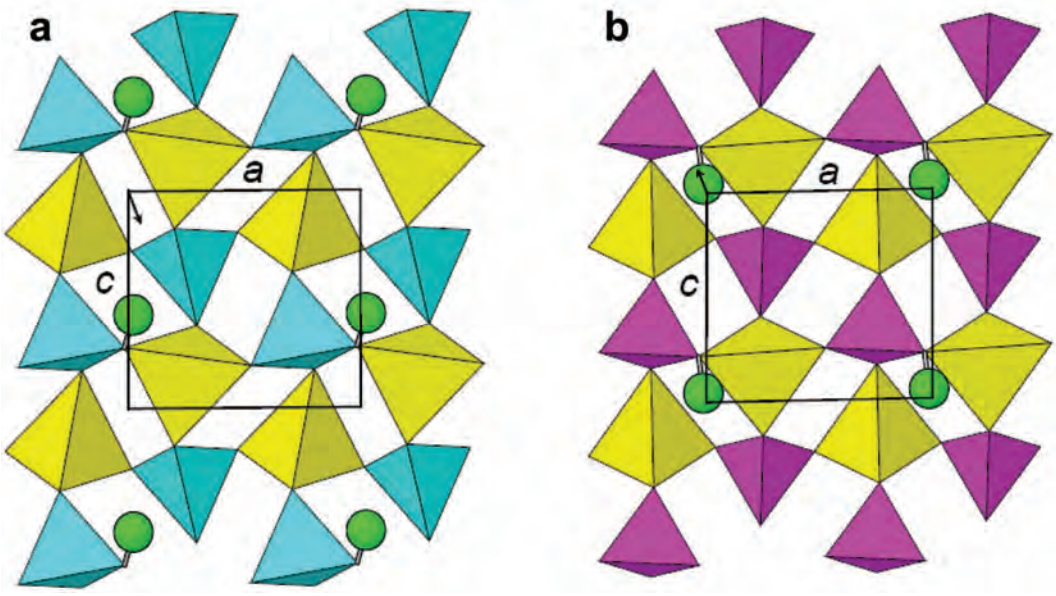

FIG. 2. Part of the crystal structures of (*a*) davidlloydite and (*b*) parahopeite projected onto (010), showing the connectivity of the ($Zn(2)O_4$) tetrahedra (yellow), the (AsO_4) tetrahedra (blue in davidlloydite) and the (PO_4) tetrahedra (pink in parahopeite) to form sheets of corner-sharing tetrahedra of the form [$ZnT^{5+}O_4$]. Green circle: $Zn(1)$ site above the [$ZnT^{5+}O_4$] sheet; the origin in parahopeite is shifted by (0, ½, 0).

parahopeite, $Zn_3(PO_4)_2(H_2O)_4$ (Chao, 1969). The details of this relation seem to be affected by the relative orientation of the structural units in the two structures (see below). Of course, this is not really the case; the structures are as they are, and their relation cannot be affected by issues of relative orientation. However, this issue is quite subtle in the present case, and is of interest, as failure to recognize such a relation could easily lead to the erroneous identification of the same structure as two distinct minerals.

Davidlloydite and parahopeite as stacking variants

In the crystal structure of davidlloydite, ZnO_4 and AsO_4 tetrahedra share corners to form a sheet (Fig. 2*a*) of the form [$ZnAsO_4$] in which the cations occur at the vertices of a 4_4 net. This sheet is topologically identical to the [$ZnPO_4$] sheet in parahopeite (Fig. 2*b*). In both davidlloydite and parahopeite, the sheets stack in the *b* direction (Fig. 3) and are linked by sharing corners with $ZnO_2(H_2O)_4$ octahedra. The position of $^{[6]}Zn$ above the sheet differs in each structure (Fig. 2): it is located at 0 ½ 0 in parahopeite and 0 ½ ½ in davidlloydite. As a result, the sense of the translational repeat in the *b* direction is different in each structure (Fig. 3). This results in a seemingly different linkage between the [$ZnTO_4$] sheets in each structure. As is apparent in Fig. 3, the $ZnO_2(H_2O)_4$ octahedra linking adjacent sheets are inclined to the right in davidlloydite (Fig. 3*a*) and to the left in parahopeite (Fig. 3*b*), and these different linkages impart quite different degrees of geometrical distortion to the constituent layers (Fig. 2).

Davidlloydite as an inverse parahopeite structure

We may select a different unit cell for davidlloydite that is geometrically congruent to that of parahopeite. The matrix transformation between the two orientations of davidlloydite is [−1 0 0 / 0 1 0 / 0 0 −1]. In this orientation, the unit cells and site coordinates of davidlloydite and parahopeite are congruent (Table 8). The only apparent difference between the two structures is the distinction in cation identity at the two tetrahedrally coordinated sites; the locations of the pentavalent and divalent cations appear interchanged in the two structures (Fig. 4).

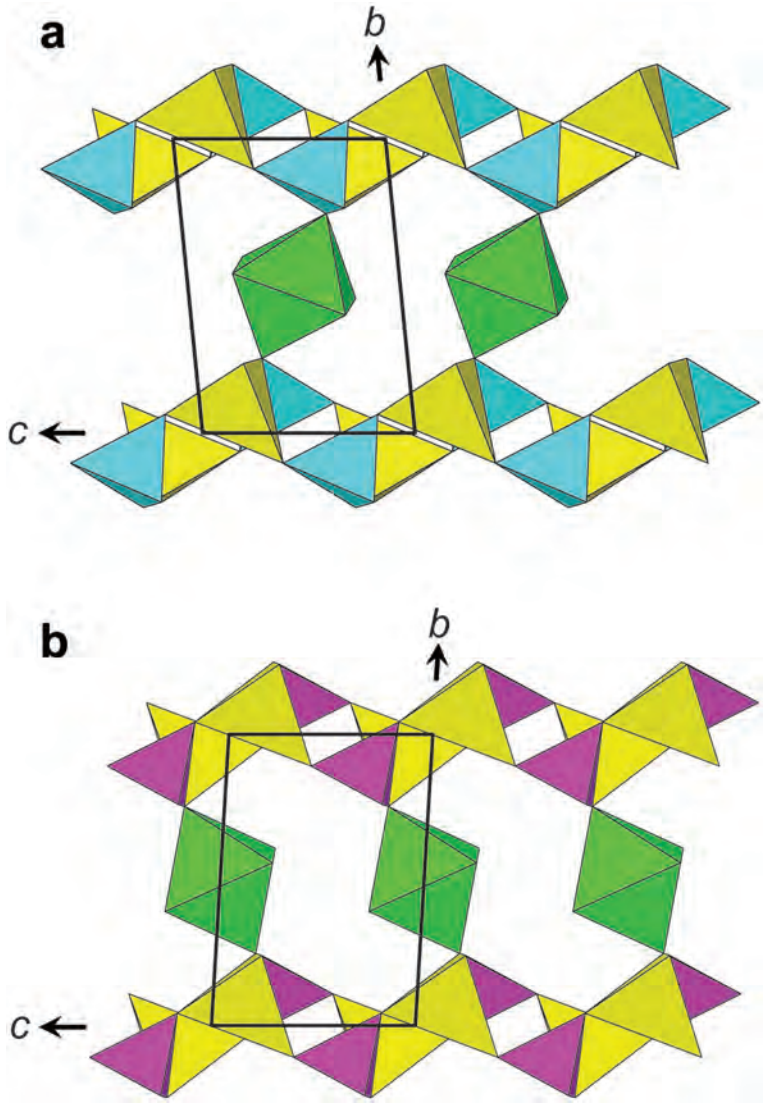

FIG. 3. The crystal structure of (*a*) davidlloydite and (*b*) parahopeite projected along [100], showing the stacking of the $[ZnT^{5+}O_4]$ sheets in the *b* direction. The ($Zn(2)O_4$) tetrahedra are yellow, the (AsO_4) tetrahedra are blue in davidlloydite and the (PO_4) tetrahedra are pink in parahopeite, *Zn*(1) octahedra are green.

FIG. 4 (*facing page*). All three principal axial projections (*a*, *c*, *e*) for davidlloydite transformed via [−1 0 0 / 0 1 0 / 0 0 −1] and (*b*, *d*, *f*) parahopeite. The ($Zn(2)O_4$) tetrahedra are yellow, the (AsO_4) tetrahedra are blue in davidlloydite and the (PO_4) tetrahedra are pink in parahopeite, *Zn*(1) octahedra are green. The origin for the parahopeite structure is that used by Chao (1969).

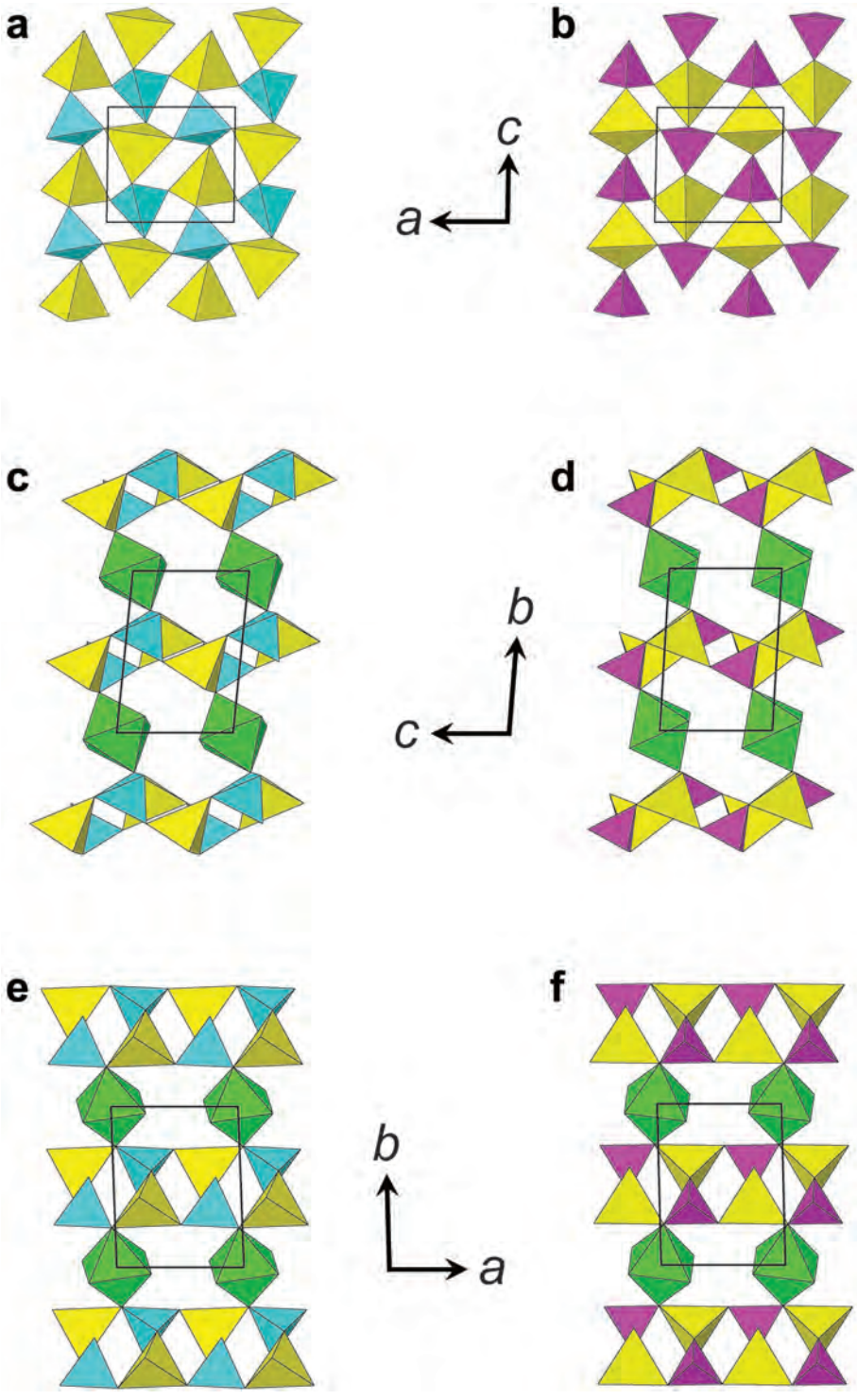
a
c
a
b
b
c
c
d
e
b
a
f

TABLE 8. Davidlloydite and parahopeite analogous cell and structure comparison.

	Davidlloydite			Parahopeite		
a (Å)	5.976			5.768		
b	7.600			7.550		
c	5.447			5.276		
α (°)	95.71			93.42		
β	90.49			91.18		
γ	92.00			91.37		
V (Å^3)	246.0			229.2		
	x/*a*	*y*/*b*	*z*/*c*	*x*/*a*	*y*/*b*	*z*/*c*
Zn(1)	0	0	0	0	0	0
As / *Zn*(2)	0.259	0.630	0.837	0.252	0.598	0.817
Zn(2) / *P*	0.239	0.396	0.311	0.250	0.362	0.296
O(1)	0.519	0.264	0.274	0.468	0.259	0.227
O(2)	0.195	0.437	0.667	0.233	0.391	0.586
O(3)	−0.027	0.246	0.186	0.029	0.252	0.197
O(4)	0.300	0.603	0.135	0.251	0.542	0.171
O(5)	0.271	0.958	0.283	0.230	0.891	0.261
O(6)	0.223	0.099	0.773	0.266	0.059	0.748

Hydrogen bonding in davidlloydite and parahopeite

The arrangement of the hydrogen bonds for davidlloydite is shown in Fig. 5*a*. For the H_2O group at O(5), the hydrogen bond from H(1) is directed toward the O(4) anion of the neighbouring sheet of tetrahedra, and the hydrogen bond from H(2) is directed across the interstitial region to the neighbouring O(6) anion (the other H_2O group in the structure) of the adjacent *Zn*(1) octahedron. For the H_2O group at O(6), the hydrogen bonds from H(3) and H(4) are directed toward opposing O(1) and O(2) anions, respectively, belonging to the sheets on either side of the *Zn*(1) octahedron. We have inferred the same style of hydrogen bonding for parahopeite (Fig. 5*b*). Note that the two structures differ only in the relative sense of alternating *Zn*(1) occupancy and neighbouring hydrogen bonding in the interlayer region. The stereochemistry of the donor-acceptor anions is given for the two structures in Table 9.

Related minerals

In the classification of Strunz (Strunz and Nickel, 2001), davidlloydite is a class 8 phosphate-arsenate-vanadate of the 08.CA.30 hopeite group; in the classification of Dana (Gaines *et al.*, 1997), it is a class 40 normal hydrated phosphate-arsenate-vanadate related to parahopeite (Kumbasar and Finney, 1968) (40.3.3.1) and hopeite (Hill and Jones, 1976) (40.3.4.1). Structurally, davidlloydite is similar to parahopeite (as discussed above) and it is a triclinic polytype of arsenohopeite (orthorhombic $Zn_3(AsO_4)_2(H_2O)_4$, Neuhold *et al.*, 2011). Arsenohopeite is the arsenate analogue of hopeite. The structural relations between parahopeite (Kumbasar and Finney, 1968) and hopeite

TABLE 9. Donor-acceptor anion distances (Å) and angles (°) for the hydrogen bonding in davidlloydite and parahopeite.

	Davidlloydite	Parahopeite
O(5)···O(4)	2.70	2.66
O(5)···O(6)	2.79	2.80
O(4)−O(5)−O(6)	95.2	123.3
O(6)···O(1)	2.72	2.89
O(6)···O(2)	2.75	2.71
O(1)−O(6)−O(2)	139.4	148.1

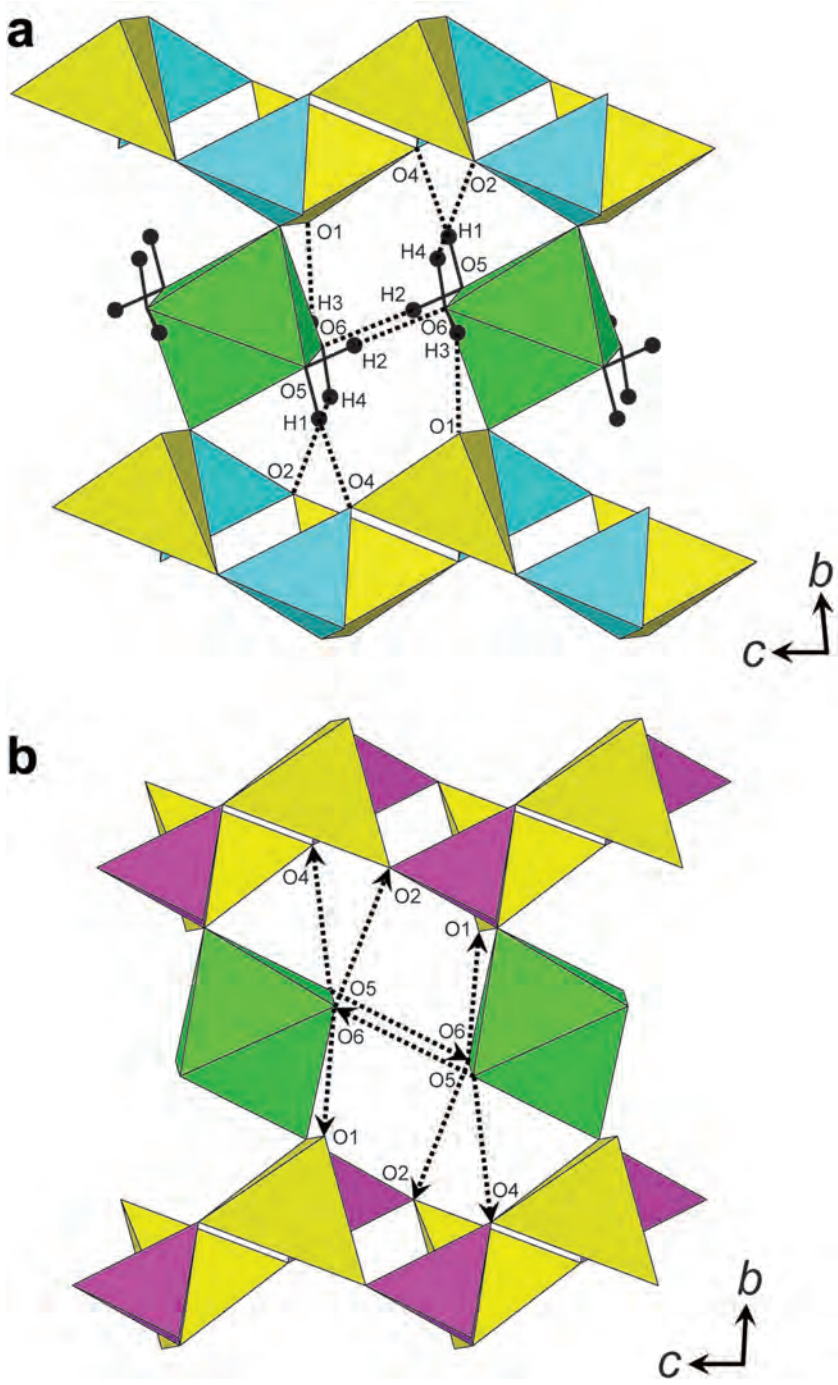

FIG. 5. Hydrogen bonding in (*a*) davidlloydite and proposed hydrogen-bonding in (*b*) parahopeite projected down an axis rotated slightly from [100]. The ($Zn(2)O_4$) tetrahedra are yellow, the (AsO_4) tetrahedra are blue in davidlloydite and the (PO_4) tetrahedra are pink in parahopeite, *Zn*(1) octahedra are green.

TABLE 10. Comparative table for selected minerals of the hopeite group.

	Davidlloydite	Parahopeite	Hopeite	Arsenohopeite*
Formula	$Zn_3(AsO_4)_2(H_2O)_4$	$Zn_3(PO_4)_2(H_2O)_4$	$Zn_3(PO_4)_2(H_2O)_4$	$Zn_3(AsO_4)_2(H_2O)_4$
Symmetry	Triclinic	Triclinic	Orthorhombic	Orthorhombic
Space group	$P\bar{1}$	$P\bar{1}$	*Pnma*	*Pnma*
a (Å)	5.9756	5.768	10.594	10.804
b (Å)	7.6002	7.550	18.333	19.003
c (Å)	5.4471	5.296	5.029	5.112
α (º)	84.2892	93.42	90	90
β (º)	90.4920	91.18	90	90
γ (º)	87.9958	91.37	90	90
Z	1	1	4	4
d (g cm^{-3})	3.661	3.32	2.94	3.46
Colour	Colourless	Colourless	Colourless to greyish white	–
Cleavage	{010} distinct	{010} perfect	{010} perfect, {100} good, {001} poor	–
Hardness	3–4	3½–4	3½	–
Occurrence	Cu-Zn deposits	Cu-Zn deposits	Cu-Zn deposits	–

* From Neuhold *et al.* (2011).

were discussed by Hill and Jones (1976). Selected properties of davidlloydite, parahopeite, hopeite and arsenohopeite are listed in Table 10. Other minerals of the form $(M^{2+})_3(T^{5+}O_4)_2(H_2O)_4$, such as phosphophyllite, $Zn_2Fe(PO_4)_2(H_2O)_4$; ludlamite, $Fe_3(PO_4)_2(H_2O)_4$ and rollandite, $Cu_3(AsO_4)_2(H_2O)_4$, have different M-coordination environments (i.e. not $^{[6]}M\ ^{[4]}M_2$) and represent structural variants (Hill, 1977; Abrahams and Bernstein, 1966; Sarp and Černy, 2000).

Triclinic polytypism in davidlloydite and parahopeite

The tetrahedral $[ZnAsO_4]$ sheet in davidlloydite displays minor rotation of the tetrahedra relative to the $[ZnPO_4]$ sheet in parahopeite (Fig. 2), and the general freedom inherent in the simple corner linkage of tetrahedra seems to easily accommodate the difference in radius of $^{[4]}As^{5+}$ and $^{[4]}P$. The similar patterns of intersheet linkage by interstitial $ZnO_4(H_2O)_2$ octahedra and associated hydrogen bonding (Fig. 3) have the general appearance of being compatible in both structures. This suggests that two different triclinic polytypes may be possible for both davidlloydite and parahopeite; however, the diffraction characteristics for both minerals suggest simple ordered structures, rather than disordered mixtures of polytypes.

Acknowledgements

We thank Tony Kampf and an anonymous reviewer for their comments on this paper. This work was supported by a Canada Research Chair in Crystallography and Mineralogy and by Natural Sciences and Engineering Research Council of Canada Discovery, Equipment and Major Installation grants of the Natural Sciences and Engineering Research Council of Canada, and by Innovation grants from the Canada Foundation for Innovation to FCH.

References

Abrahams, S.C. and Bernstein, J.L. (1966) Crystal structure of paramagnetic ludlamite, $Fe_3(PO_4)_2{\cdot}4(H_2O)$, at 298ºK. *Journal of Chemical Physics*, **44**, 2223–2229.

Bartelmehs, K.L., Bloss, F.D., Downs, R.T. and Birch, J.B. (1992) Excalibr II. *Zeitschrift für Kristallographie*, **199**, 186–196.

Brown, I.D. and Altermatt, D. (1985) Bond-valence parameters obtained from a systematic analysis of the inorganic crystal structure database. *Acta Crystallographica*, **B41**, 244–247.

Chao, G.Y. (1969) Refinement of the crystal structure of parahopeite. *Zeitschrift für Kristallographie*, **130**, 261–266.

Gaines, R.V., Skinner, H.C.W., Foord, E.E., Mason, B. and Rosenwieg, A. (1997) *Dana's New Mineralogy*,

Eighth Edition. Wiley and Sons, New York, USA.

Hawthorne, F.C. (1976*a*) Refinement of the crystal structure of adamite. *The Canadian Mineralogist*, **14**, 143–148.

Hawthorne, F.C. (1976*b*) The hydrogen positions in scorodite. *Acta Crystallographica*, **B32**, 2891–2892.

Hill, R.J. (1977) The crystal structure of phosphophyllite. *American Mineralogist*, **62**, 812–817.

Hill, R.J. and Jones, J.B. (1976) The crystal structure of hopeite. *American Mineralogist*, **61**, 987–995.

Kumbasar, I. and Finney, J.J. (1968) The crystal structure of parahopeite. *Mineralogical Magazine*, **36**, 621–624.

Neuhold, F., Kolitsch, U., Bernhardt, H.-J. and Lengauer, C.L. (2011) Arsenhopeite, IMA 2010-69. CNMNC Newsletter No. 8, April 2011, page 291; *Mineralogical Magazine*, **75**, 289–294.

Pinch, W.W. and Wilson, W.E. (1977) Tsumeb V. Minerals: a descriptive list. *Mineralogical Record*, **8**(3), 17–37.

Pouchou, J.L. and Pichoir, F. (1985) 'PAP' φ(ρZ) procedure for improved quantitative microanalysis. Pp. 104–106 in: *Microbeam Analysis* (J.T. Armstrong, editor). San Francisco Press, San Francisco, California, USA.

Sarp, H. and Cerný, R. (2000) Rollandite, $Cu_3(AsO_4)_2{\cdot}4H_2O$, a new mineral: its description and crystal structure. *European Journal of Mineralogy*, **12**, 1045–1050.

Sheldrick, G.M. (2008) A short history of *SHELX*. *Acta Crystallographica*, **A64**, 112–122.

Strunz, H. and Nickel, E.H. (2001) *Strunz Mineralogical Tables*, Ninth Edition. Schweizerbart'sche Verlagsbuchhandlung, Stuttgart, Germany.

Weber, D. and Wilson, W.E. (1977) Tsumeb IV. Geology. *Mineralogical Record*, **8**(3), 14–16.